Environmental Science & Technology

pubs.acs.org/est

Article

Peracetic Acid Enhances Micropollutant Degradation by Ferrate(VI) through Promotion of Electron Transfer Efficiency

Junyue Wang, Juhee Kim, Daniel C. Ashley, Virender K. Sharma,* and Ching-Hua Huang*

Cite This: *Environ. Sci. Technol.* 2022, 56, 11683−11693

Read Online

ACCESS | Metrics & More | Article Recommendations | Supporting Information

ABSTRACT: Ferrate(VI) and peracetic acid (PAA) are two oxidants of growing importance in water treatment. Recently, our group found that simultaneous application of ferrate(VI) and PAA led to much faster degradation of micropollutants compared to that by a single oxidant, and this paper systematically evaluated the underlying mechanisms. First, we used benzoic acid and methyl phenyl sulfoxide as probe compounds and concluded that Fe(IV)/Fe(V) was the main reactive species, while organic radicals [$CH_3C(O)O^{\bullet}$/$CH_3C(O)OO^{\bullet}$] had negligible contribution. Second, we removed the coexistent hydrogen peroxide (H_2O_2) in PAA stock solution with free chlorine and, to our surprise, found the second-order reaction rate constant between ferrate(VI) and PAA to be only about $1.44 \pm 0.12\ M^{-1}s^{-1}$ while that of H_2O_2 was as high as $(2.01 \pm 0.12) \times 10^1\ M^{-1}s^{-1}$ at pH 9.0. Finally, further experiments on ferrate(VI)-bisulfite and ferrate(VI)-2,2′-azino-bis(3-ethylbenzothiazoline-6-sulfonic)acid systems confirmed that PAA was not an activator for ferrate(VI). Rather, PAA could enhance the oxidation capacity of Fe(IV)/Fe(V), making their oxidation outcompete self-decay. This study, for the first time, reveals the ability of PAA to promote electron transfer efficiency between high-valent metals and organic contaminants and confirms the benefits of co-application of ferrate(VI) and PAA for alkaline wastewater treatment.

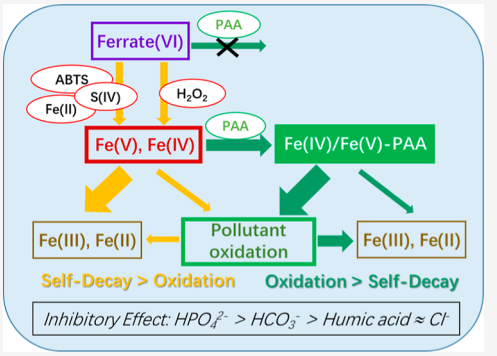

KEYWORDS: *ferrate(VI), peracetic acid, advanced oxidation, water treatment, Fe(IV)/Fe(V), multi-oxidant system*

INTRODUCTION

Pollution by pathogens and trace organic contaminants [e.g., pharmaceuticals and personal care products (PPCPs)] poses considerable threats to urban water quality and public health.[1] To control the risks, multiple strong oxidants have been developed in the past decades for water/wastewater treatment. So far, free chlorine is the most commonly used oxidant,[2] while monochloramine,[3] ozone,[4] and chlorine dioxide[5] are also applied in some treatment facilities. However, these oxidants each bear some demerits. In particular, formation of unwanted oxidation products and disinfection byproducts (DBPs) has raised public concerns.[6,7] For example, free chlorine leads to the formation of trihalomethanes, haloacetic acids, haloacetaldehydes, and haloacetonitriles.[2,7,8] Monochloramine triggers the production of *N*-nitrosamines and haloacetamides.[9−11] Ozone is the main contributor to generating bromate and nitromethanes.[12,13] All of the above-mentioned are toxic or carcinogenic byproducts. Consequently, research interests in alternative oxidants that produce less or no harmful DBPs have remained and continued to increase.

Ferrate(VI) [Fe(VI), $HFeO_4^-$/FeO_4^{2-}][14−16] and peracetic acid [PAA, $CH_3C(O)OOH$][17,18] are two promising alternative oxidants that are attracting growing interest from environmental engineers and scientists due to their great capacity for pathogen inactivation[19−23] and micropollutant abatement.[18,24−27] Nonetheless, ferrate(VI) and PAA both undergo self-decay under environmentally relevant conditions, and their reactivity toward certain contaminants is limited.[18,28−30] Thus, various methods for enhancing the oxidation ability of PAA and ferrate(VI) have been developed in recent years. For example, UV,[31,32] Fe(II),[33] Fe(III)-picolinic acid-,[34] Co(II),[35−37] Ru(III),[38] MoS_2,[39] and Co-based catalysts[40−42] have been developed to activate PAA. These PAA-based advanced oxidation processes (AOPs) efficiently degrade various PPCPs, in which organic radicals [e.g., $CH_3C(O)O^{\bullet}$/$CH_3C(O)OO^{\bullet}$] and high-valent metals [e.g., Fe(IV), Co(IV)] are proposed as the major reactive species. Despite these findings, it is difficult for the Fe(II)-PAA process to achieve high efficiency at neutral to alkaline pHs,[33] while the Co-, Ru-, and Mo-based systems depend on expensive metals and material synthesis. For ferrate(VI), spiking of Fe(III) ions,[43] silicate,[44] ammonia,[45] and bicarbonate[46] has shown a beneficial impact for activating ferrate(VI) oxidation of PPCPs. However,

Received: April 5, 2022
Revised: July 7, 2022
Accepted: July 8, 2022
Published: July 26, 2022

Table 1. Reactions in the Ferrate(VI)-PAA System and the Second-Order Rate Constants at pH 9.0[a]

no	reactions	k ($M^{-1}s^{-1}$)	ref
R1	$Fe(VI) + H_2O \rightarrow Fe(IV) + H_2O_2$	2.00×10^{-5}	43
R2	$Fe(VI) + H_2O_2 \rightarrow Fe(IV) + O_2$	$(2.01 \pm 0.12) \times 10^{1}$	Figure 3a
R3	$2\ Fe(IV) \rightarrow 2\ Fe(III) + H_2O_2$	1.00×10^{7}	43
R4	$Fe(IV) + H_2O_2 \rightarrow Fe(II) + O_2$	3.00×10^{3}	43
R5	$Fe(IV) + Fe(II) \rightarrow 2\ Fe(III)$	1.00×10^{6}	43
R6	$Fe(II) + H_2O_2 \rightarrow Fe(IV)$	1.00×10^{3}	43
R7	$Fe(VI) + Fe(II) \rightarrow Fe(III) + Fe(V)$	1.00×10^{5}	43
R8	$Fe(V) + H_2O \rightarrow Fe(III) + H_2O_2$	5.00	43
R9	$2\ Fe(V) \rightarrow 2\ Fe(III) + 2\ H_2O_2$	1.50×10^{7}	43
R10	$Fe(V) + H_2O_2 \rightarrow Fe(III) + O_2$	4.00×10^{5}	43
R11	$Fe(VI) + PAA \rightarrow Fe(IV) + Ac^- + O_2$	1.44 ± 0.12	Figure 3a
R12	$Fe(IV) + PAA \rightarrow [Fe(IV)\text{-}PAA] \rightarrow Fe(II) + Ac^- + O_2$[a]	unknown[b]	
R13	$Fe(V) + PAA \rightarrow [Fe(V)\text{-}PAA] \rightarrow Fe(III) + Ac^- + O_2$	unknown[b]	
R14	$Fe(VI) + PAA \rightarrow Fe(V) + CH_3COOO^{\bullet}$	negligible[b]	Figure 2

[a]Ac^- = acetate. [b]R12−14 were not included in the kinetic modeling.

the enhancing effect occurs at a high concentration of anions (e.g., bicarbonate) which are present in special matrices such as hydrolyzed urine. So far, bisulfite (HSO_3^-) appears to be among the most promising activators for ferrate(VI); however, one drawback is that HSO_3^- also reacts very quickly with generated high-valent iron species [Fe(IV)/Fe(V)] and causes the loss in oxidant utilization efficiency.[47,48]

More recently, our team found that simultaneous application of ferrate(VI) (200 μM) and PAA (100 μM) could degrade multiple PPCPs by 80−90% in less than 1 min at pH 9.0,[49] faster than most other activated ferrate(VI) or activated PAA systems under alkaline conditions. It was the first report of such a multi-oxidant system with high performance. In the previous study, Fe(IV)/Fe(V) and $CH_3C(O)O^{\bullet}$/$CH_3C(O)OO^{\bullet}$ were hypothesized to be the reactive species, but the reaction mechanism was not confirmed. In this study, our aim was to delineate the mechanism of how PAA accelerates PPCP oxidation by ferrate(VI). A range of approaches were employed including investigating suitable probe compounds, developing a reliable method to measure PAA in the presence of ferrate(VI), kinetic modeling, and oxidation product analysis. Additionally, the ferrate(VI)-PAA reaction system was evaluated for the impacts of water matrix constituents. As will be discussed later, surprisingly, PAA reacts with ferrate(VI) rather slowly. The results revealed mechanistic insights that were not recognized in the previous literature and led to the proposing of a new reaction mechanism.

MATERIALS AND METHODS

Chemicals and Reagents. PAA solution (32% PAA and 6% H_2O_2 w/w in acetic acid and water solution) and hydrogen peroxide solution (30% H_2O_2 w/w in water) were obtained from Sigma-Aldrich (St. Louis, MO), and the oxidant concentrations were determined by titration methods.[33] Carbamazepine (CBZ), benzoic acid (BA), and methyl phenyl sulfoxide (PMSO), chosen as representative contaminants, were acquired from Sigma-Aldrich. Other chemicals used in this study are listed in Supporting Information Text S1.

Ferrate(VI)-PAA Experiments. Ferrate(VI) stock solution was prepared within 30 min of all the experiments and buffered at pH 9.2 with borate (1 mM).[29,50] Then, ferrate(VI) solution was mixed with the working solution containing the target contaminant and freshly prepared PAA and/or H_2O_2 solution in a 100 mL beaker. Background anions, humic acid (HA), $NaHSO_3$, and acetate were added [prior to ferrate(VI)] where noted. All batch experiments were conducted with constant magnetic stirring at room temperature and open to the ambient air. Solution pH was buffered by borate, monitored throughout the reaction, and adjusted by NaOH (1 M) and/or H_2SO_4 (1:3 v/v in DI water) if necessary. To monitor contaminant degradation over time, 1 mL aliquots were taken from the reactor into amber high-performance liquid chromatography (HPLC) glass vials at selected time intervals and quenched immediately by 0.1 mL of $Na_2S_2O_3$ (500 mM).[51]

In selected experiments, coexistent H_2O_2 in PAA stock solution was quenched by free chlorine to create a "H_2O_2-free" PAA solution prior to further tests, where the free chlorine and H_2O_2 concentrations were both below 1% of the PAA concentration (see detailed description in Supporting Information Text S2). In this paper, the coexistent H_2O_2 concentrations in all experiments were always clearly noted with the data.

UV/PAA Experiments. In order to test the reactivity of probe compounds toward the organic radicals, UV/PAA experiments were conducted using a cylindrical quartz reactor in a chamber equipped with a 4 W low-pressure UV lamp (G4T5 Hg lamp, Philips TUV4W).[32] The reactor was stirred magnetically and open to the ambient air. Periodically, 1.0 mL samples were taken and immediately quenched by $Na_2S_2O_3$.

Analytical Methods. The target organic compounds were measured by HPLC equipped with a diode array detector (HPLC-DAD) (Supporting Information Text S3). The oxidation products of CBZ were analyzed by liquid chromatography−high-resolution mass spectrometry (LC-HRMS), with electrospray ionization (ESI) and a time-of-flight mass analyzer, after solid phase extraction (Supporting Information Text S4). The ferrate(VI) concentration was measured by either absorbance at 510 nm or by the 2,2′-azino-bis(3-ethylbenzothiazoline-6-sulfonic)acid (ABTS) method.[52] For the latter, 0.2 mM ABTS stock solution was freshly prepared in 100 mM phosphate buffer solution at pH 7.0, under which condition the ferrate(VI) consumption and $ABTS^{\bullet+}$ generation were reported to be 1:1 even when ABTS is in excess (confirmed in this study).[52,53] Sample aliquots (1.0 mL) were added into 9.0 mL of ABTS solution, and the absorbance was immediately measured at 415 nm for $ABTS^{\bullet+}$ using a UV−visible spectrophotometer.[52] Free

https://doi.org/10.1021/acs.est.2c02381
Environ. Sci. Technol. 2022, 56, 11683−11693

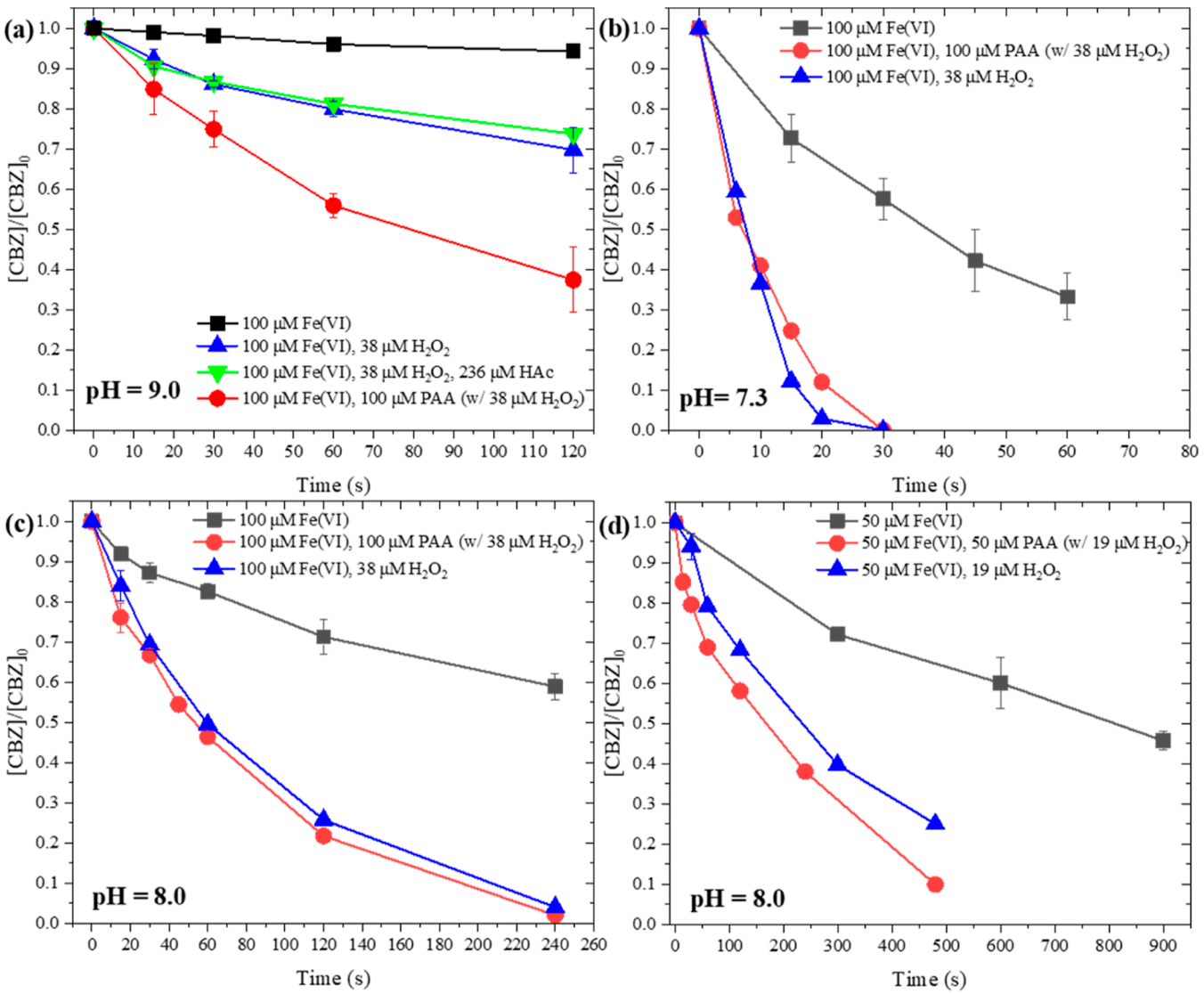

Figure 1. CBZ degradation by ferrate(VI), ferrate(VI)−H_2O_2, and ferrate(VI)-PAA at pH 9.0 (a), 7.3 (b), and 8.0 (c,d). Experimental conditions: $[CBZ]_0$ = 10 μM, [borate buffer] = 10 mM, pH = 7.3 ± 0.1, 8.0 ± 0.1, and 9.0 ± 0.1, as noted, and temperature = 23 ± 2 °C. Error bars represent standard deviation between parallel experiments. HAc = acetic acid.

chlorine was measured by the *N,N*-diethyl-*p*-phenylenediamine (DPD) method,[54] while the H_2O_2 concentration was measured by the Ti(IV) sulfate method.[55] Note that the direct reaction of DPD with PAA and H_2O_2 in the sample was negligible during measurement of free chlorine. To measure PAA in the presence of ferrate(VI), an ABTS−DPD−KI method was developed (to be discussed later).

Kinetic Model Simulation. The kinetic model simulations were performed using Kintecus 4.55.31 (Table 1). The goodness of fit between simulation and experimental data was quantified by calculating the normalized root mean square deviation (details in Supporting Information Text S5).

RESULTS AND DISCUSSION

CBZ Degradation by Ferrate(VI)-PAA at Different pHs. Commercial PAA solutions contain PAA, H_2O_2, acetic acid, and water.[18] In the ferrate(VI)-PAA system, the potential impacts of PAA, H_2O_2, and acetic acid on ferrate(VI) reactivity should all be considered. Through separate investigations with PAA, H_2O_2, and acetic acid, our previous study demonstrated that PAA promoted the degradation of PPCPs (including CBZ) by ferrate(VI) at pH 9.0 much more significantly than coexistent H_2O_2, while the coexistent acetate exerted little promoting effect.[49] The promoting effect of H_2O_2 on contaminant degradation by ferrate(VI) has been well documented.[30] Briefly, H_2O_2 can activate ferrate(VI) through R2 (Table 1) to generate Fe(IV) and subsequently Fe(V), and both Fe(IV)/(V) are much more reactive with organic compounds than ferrate(VI).[56,57]

In the present study, we evaluated the reaction in an additional pH range (7.3−9.0). As shown in Figure 1, CBZ oxidation was significantly enhanced by adding equimolar ferrate(VI) and PAA at pH 7.3−9.0, compared with oxidation by ferrate(VI) only. However, we also found that similar CBZ degradation could be achieved by adding only the amount of coexistent H_2O_2 at pH 7.3 and 8.0. In other words, the enhancing effect of PAA on ferrate(VI) oxidation at pH 7.3 and 8.0 was mostly due to coexistent H_2O_2, instead of PAA itself. In contrast, at pH 9.0, an obvious additional acceleration effect of PAA was observed compared with coexistent H_2O_2

https://doi.org/10.1021/acs.est.2c02381
Environ. Sci. Technol. 2022, 56, 11683−11693

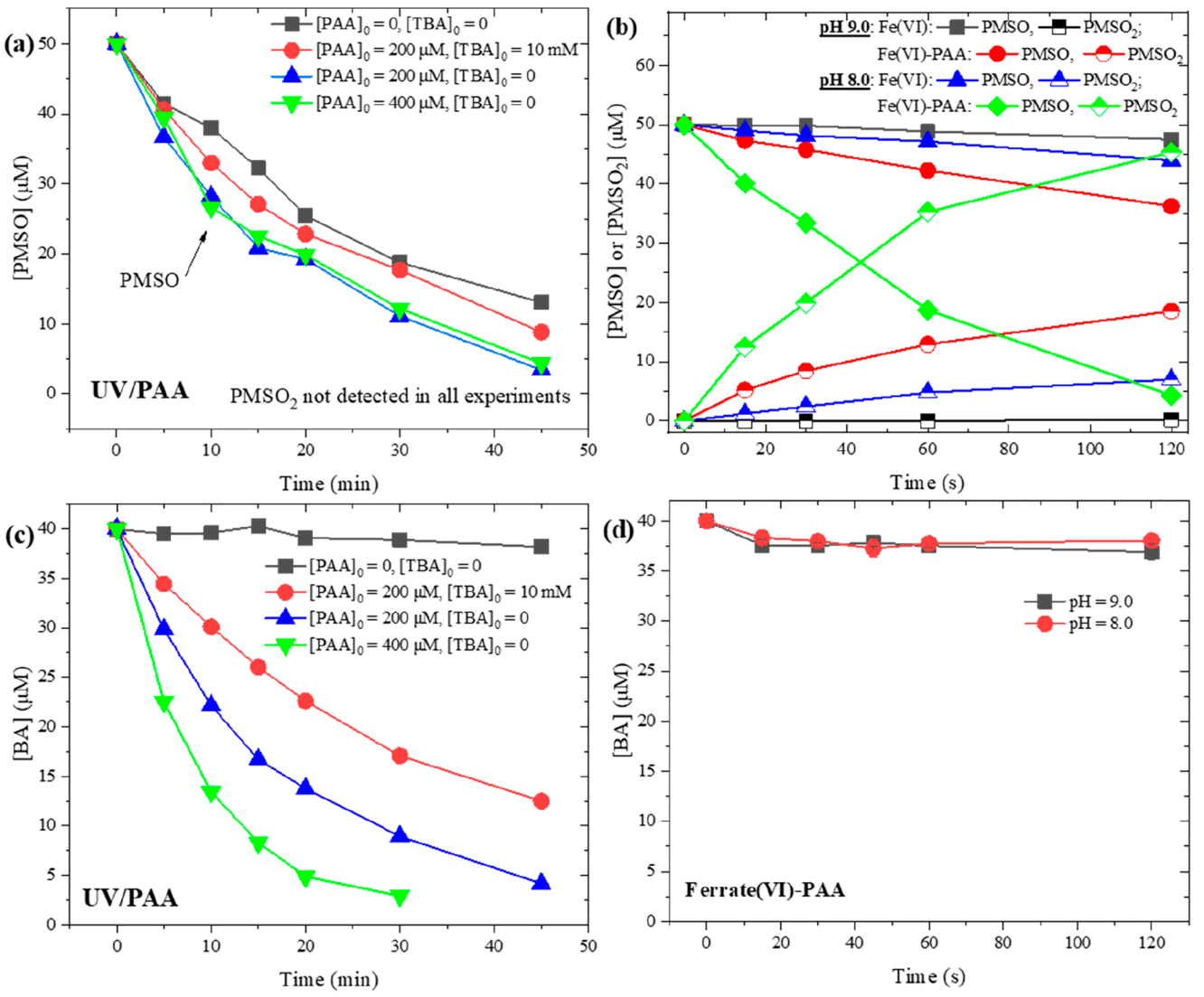

Figure 2. PMSO (a,b) and BA (c,d) degradation by UV/PAA (a,c) and ferrate(VI)-PAA (b,d). Experiment conditions: $[BA]_0$ = 40 μM, $[PMSO]_0$ = 50 μM, and temperature = 23 ± 2 °C; for a, c, pH = 6.0 ± 0.1, [phosphate buffer] = 10 mM, and coexistent $[H_2O_2]_0$ = 0.38 $[PAA]_0$; and for b,d, [ferrate(VI)]$_0$ = 100 μM, $[PAA]_0$ = 100 μM (w/38 μM coexistent H_2O_2), [borate buffer] = 10 mM, and pH as noted. Error bars represent standard deviation between parallel experiments. Some data of Figure 2c also appeared in the Supporting Information of ref 34.

(Figure 1a). The pH difference is likely related to PAA speciation in that only the deprotonated PAA (pK_a = 8.2[18]) may contribute to CBZ degradation by ferrate(VI). The above-mentioned results also indicate that PAA can be applied together with ferrate(VI) particularly in wastewaters with higher pH (e.g., alkaline industrial wastewater, hydrolyzed urine[46,58]) to achieve efficient decontamination. However, the beneficial effect of PAA on ferrate(VI) at pH ≤ 8.0 would not be obvious compared with the addition of H_2O_2.

The mechanism of how deprotonated PAA accelerates ferrate(VI) oxidation of contaminants was still unknown. Initially, we hypothesized that PAA acted as an activator like H_2O_2. As a result, R11 and R14 in Table 1 were suggested in our previous study for the potential involvement of PAA.[49] This hypothesis was evaluated in this study (see later discussion) to discern the role of PAA in the ferrate(VI)-PAA system.

Reactive Species in the Ferrate(VI)-PAA System. Probe compounds and quencher tests have been widely applied for the purpose of distinguishing different reactive species. The selection of quenchers and probes is crucial for a correct conclusion. Therefore, commonly used quenchers and probes in PAA-related AOPs are discussed in detail below.

TBA and 2,4-Hexadiene as Quenchers for Metal-PAA Systems. *tert*-Butyl alcohol (TBA) and 2,4-hexadiene were used to verify the roles of organic radicals in metal-PAA systems.[32,36] TBA is known to be a selective quencher for the hydroxyl radical (•OH), while 2,4-hexadiene quenches both •OH and organic radicals [i.e., $CH_3C(O)O^•$/$CH_3C(O)$-$OO^•$].[31] When TBA exhibits no effect while 2,4-hexadiene inhibits PPCP degradation in a PAA-AOP, it may be concluded that the organic radicals are involved.[36,38,49] However, the reactivity of 2,4-hexadiene with high-valent metals [e.g., Fe(IV)/Fe(V), Co(IV), Ru(IV), and Ru(V)] remains unknown. Thus, 2,4-hexadiene alone is insufficient to confirm the organic radicals (R-O•) in systems where high-valent metal species could also be present.

CBZ as a Probe Compound for Metal-PAA Systems. CBZ has been used as a probe in Co(II)-PAA AOPs to verify the role of Co(IV).[35,37] In those studies, CBZ was assumed to be

https://doi.org/10.1021/acs.est.2c02381
Environ. Sci. Technol. 2022, 56, 11683−11693

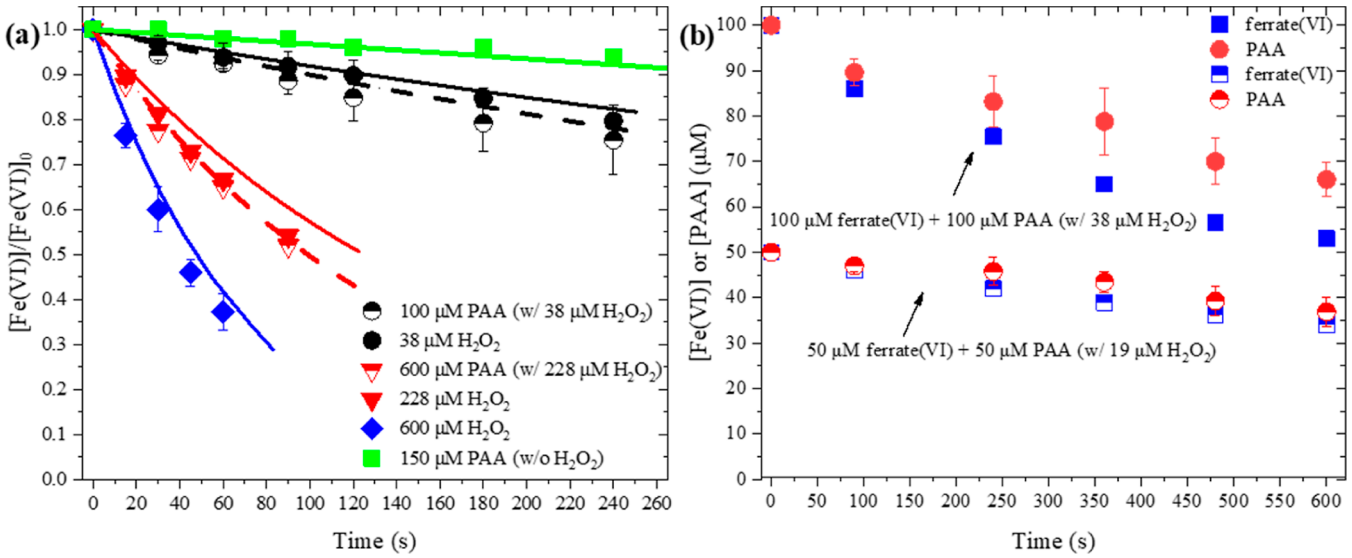

Figure 3. Degradation of 50 μM ferrate(VI) in the presence of PAA and/or H_2O_2 (a) and ferrate(VI) and PAA decay in the ferrate(VI)-PAA system (b). Experiment conditions: pH = 9.0 ± 0.1, [borate buffer] = 10 mM, and temperature = 23 ± 2 °C. Error bars represent standard deviation between parallel experiments. Solid lines represent the kinetic modeling for ferrate(VI) decay with only PAA or only H_2O_2, while dashed lines are for modeling the systems with both PAA and H_2O_2.

unreactive with the organic radicals (R-O$^\bullet$) because it could not be degraded in UV/PAA/TBA or heat-activated PAA systems.[35,37] However, these conclusions are debatable. It is noteworthy that there are several kinds of organic radicals in PAA-based AOPs, including $CH_3C(O)O^\bullet$ and its degradation products (e.g., $^\bullet CH_3$, and $^\bullet OOCH_3$) and $CH_3C(O)OO^\bullet$ (eqs 1−4).[32] Their chemical properties differ significantly and hence deserve separate consideration. In particular, oxidation of PAA by $^\bullet OH$ is an important pathway for $CH_3C(O)OO^\bullet$ generation in a UV/PAA system (eq 4).[32] Therefore, $CH_3C(O)OO^\bullet$ is also greatly removed with the addition of TBA because its precursor (i.e., $^\bullet OH$) is quenched. The negligible removal of CBZ in the UV/PAA/TBA system confirms the low reactivity of CBZ toward $CH_3C(O)O^\bullet$ and its degradation products (e.g., $^\bullet CH_3$ and $^\bullet OOCH_3$) but does not necessarily rule out $CH_3C(O)OO^\bullet$ completely. Actually, $CH_3C(O)OO^\bullet$ probably has a non-negligible reactivity toward CBZ because CBZ removal in UV/PAA was shown to exceed the possible contribution from the modeled steady-state concentration of $^\bullet OH$.[32]

$$CH_3C(O)OOH \xrightarrow{UV} CH_3C(O)O^\bullet + {}^\bullet OH \quad (1)$$

$$CH_3C(O)O^\bullet \rightarrow {}^\bullet CH_3 + CO_2 \quad (2)$$

$$^\bullet CH_3 + O_2 \rightarrow {}^\bullet OOCH_3 \quad (3)$$

$$CH_3C(O)OOH + {}^\bullet OH \rightarrow CH_3C(O)OO^\bullet + OH^- \quad (4)$$

The heat-activated PAA is also not clear evidence for CBZ's inactivity toward $CH_3C(O)OO^\bullet$ because it is currently not verified whether both $CH_3C(O)O^\bullet$ and $CH_3C(O)OO^\bullet$ are involved in the heat-activated PAA process due to lack of suitable probe compounds to differentiate $CH_3C(O)O^\bullet$ versus $CH_3C(O)OO^\bullet$.[59] Thus, CBZ may not be a convincing probe compound to distinguish between the organic radicals and high-valent metals.

PMSO as a Probe Compound for Metal-PAA Systems. PMSO, whose only oxidation product by Fe(IV), Fe(V), and Co(IV) is methyl phenyl sulfone ($PMSO_2$), is another probe compound commonly used in metal-PAA systems.[33,35,37] Importantly, the reactivity of PMSO toward the organic radicals needs to be investigated. Similar to Liu et al.,[37] we found that the degradation of PMSO in UV/PAA was mainly attributed to direct photolysis (Figure 2a). In UV/PAA, PMSO removal in the UV/PAA/TBA system was almost the same as that by UV alone, suggesting that PMSO reacts with $CH_3C(O)O^\bullet$ limitedly, if at all. Doubling the PAA concentration did not lead to increased PMSO degradation. Note that owing to the mixture nature of PAA solution, doubling the applied PAA concentration also increased the concentrations of H_2O_2 and acetate proportionally. When the applied PAA concentration is doubled in UV/PAA, the steady-state concentration of $^\bullet OH$ should remain the same because (1) the $^\bullet OH$ production, approximately linear to PAA and H_2O_2 concentrations, is doubled, and (2) $^\bullet OH$ consumption [dominated by PAA (eq 4) along with impacts of acetate and H_2O_2] is also doubled. This outcome was confirmed by the work of Zhang et al., in which the steady-state concentration of $^\bullet OH$ (1.6×10^{-13} M) did not change when the applied PAA concentration was increased.[32] However, as also demonstrated in the work of Zhang et al., the concentration of $CH_3C(O)OO^\bullet$ increased significantly by doubling PAA dosage.[20,32] Therefore, the similar removal efficiency of PMSO at two PAA dosages in UV/PAA (Figure 2a) indicated the sluggish reactivity of $CH_3C(O)OO^\bullet$ with PMSO. To sum up, the tests of PMSO in the UV/PAA system confirmed that PMSO has low reactivity toward $CH_3C(O)O^\bullet$/$CH_3C(O)OO^\bullet$. Furthermore, PAA greatly enhanced PMSO oxidation by ferrate(IV), and a near 100% conversion yield of PMSO to $PMSO_2$ (Figure 2b) confirmed the existence of high-valent metals [i.e., Fe(V)/Fe(IV)] but could not confirm the absence of the organic radicals.

BA as a Probe Compound for Metal-PAA Systems. BA was identified as a better probe compound to distinguish $CH_3C(O)O^\bullet$/$CH_3C(O)OO^\bullet$ from Fe(IV)/Fe(V) in our study. It is well-acknowledged that BA is non-reactive toward Fe(IV)/Fe(V) and has been used to differentiate Fe(IV)/

https://doi.org/10.1021/acs.est.2c02381
Environ. Sci. Technol. 2022, 56, 11683−11693

Fe(V) and the sulfate radical ($SO_4^{\bullet-}$) in the ferrate(VI)−HSO_3^- process.[47,48] Then, we tested BA removal in the UV/PAA system. We found that BA is reactive toward both $CH_3C(O)O^\bullet$ and $CH_3C(O)OO^\bullet$, evidenced by BA removal in UV/PAA/TBA and the enhanced removal by doubling PAA dosage, respectively (Figure 2c). Therefore, BA could be used as a probe compound in a ferrate(VI)-PAA system. If $CH_3C(O)O^\bullet/CH_3C(O)OO^\bullet$ is generated, BA could be degraded; otherwise, BA cannot be removed due to sluggish reactivity with Fe(IV)/Fe(V). The experiments showed no degradation of BA by ferrate(VI)-PAA at pH 8.0 or 9.0 (Figure 2d).

In summary, the above-mentioned results with PMSO and BA clearly demonstrated that Fe(IV)/Fe(V) was the main oxidant in the ferrate(VI)-PAA system, and the contribution from $CH_3C(O)O^\bullet/CH_3C(O)OO^\bullet$ was negligible. These results also suggest that ferrate(VI) reacts with PAA through a two-electron transfer reaction to generate Fe(IV) (R11), rather than a single-electron transfer reaction to generate $CH_3C(O)OO^\bullet$ (R14).

Mechanism of PAA in Enhancing Ferrate(VI) Oxidation of CBZ. *Interaction of PAA with Fe(VI).* To understand the ability of PAA to generate Fe(IV) (Table 1, R11), ferrate(VI) decay in the presence of different dosages of PAA and H_2O_2 was investigated. First, ferrate(VI) decay with an excess amount of H_2O_2 was tested and used to model the second-order rate constant of R2 (Table 1). Previously, the second-order rate constant of ferrate(VI) and H_2O_2 was assumed to be ∼0 at pH 9.0 (Table 1, R2).[43,50] This conclusion could be applied to H_2O_2 generated during ferrate(VI) self-decay; however, it needs re-examination when additional H_2O_2 is dosed. In this study, we found that ferrate(VI) decay was greatly accelerated with addition of 600 μM H_2O_2 (Figure 3a). The rate constant for R2 was modeled to be around $(2.01 \pm 0.12) \times 10^1$ $M^{-1}s^{-1}$. Subsequently, ferrate(VI) decay with a specific amount of PAA was compared to that with corresponding background H_2O_2. Surprisingly, coexistent H_2O_2 in PAA solution nearly accounted for all of the accelerated ferrate(VI) decay, suggesting that PAA was actually playing a minor role in activating ferrate(VI). The kinetic model (Table 1 R1−R10) was able to predict the ferrate(VI) decay with various PAA and H_2O_2 concentrations (Figure 3a), without considering the reaction of PAA with Fe(IV)/Fe(V) (Table 1 R12−13, see later discussion). This agrees with the fact that the ferrate(VI) reduction (R2) is the rate-limiting step in the system and that R14 is assessed to be unimportant as discussed earlier.

To further make it clear, we removed coexistent H_2O_2 (38 mM) in PAA solution (100 mM) using free chlorine (Supporting Information Text S2). The amount of free chlorine added was carefully adjusted so that the final concentrations of free chlorine and H_2O_2 both became near/below the detection limit, while the concentration of PAA remained unchanged at 10 min, confirming the slow decay of PAA under the low-pH condition of the PAA solution (Supporting Information Text S2). This H_2O_2-free PAA solution was added into the ferrate(VI) solution and caused a very limited acceleration in ferrate(VI) decay. The second-order rate constant for the reaction of PAA with ferrate(VI) (R11) was modeled to be around only 1.44 ± 0.12 $M^{-1}s^{-1}$ (Figure 3a). In conclusion, coexistent H_2O_2, instead of PAA, was identified as the major activator of ferrate(VI) in the ferrate(VI)-PAA system.

Interaction of PAA with Fe(IV)/Fe(V). As PAA's reactivity toward ferrate(VI) is quite low, the enhancement of CBZ removal by ferrate(VI) (compared to the effect of background H_2O_2) can only be attributed to the interaction of PAA with Fe(IV)/Fe(V). To test this hypothesis, PAA was dosed into a ferrate(VI)−HSO_3^- system (Figure 4a). Control experiments

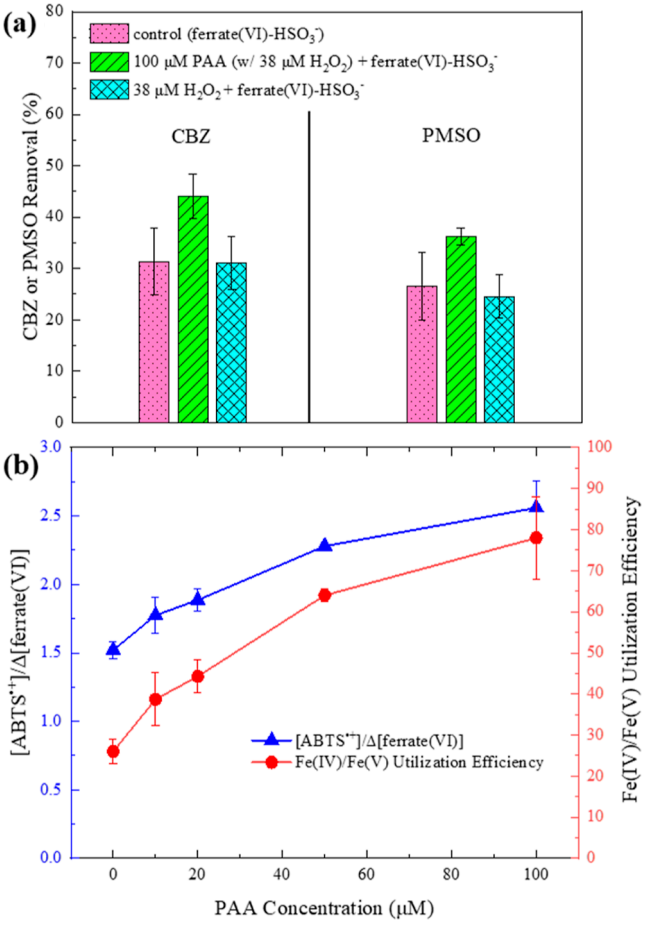

Figure 4. Impacts of PAA and H_2O_2 on CBZ and PMSO removal by the ferrate(VI)−HSO_3^- system (a) and ABTS oxidation by ferrate(VI) (b). Experiment conditions: pH = 9.0 ± 0.1, [borate buffer] = 10 mM, and temperature = 23 ± 2 °C; for a, $[ferrate(VI)]_0$ = 100 μM, $[HSO_3^-]_0$ = 20 μM, reaction time = 10 s, $[CBZ]_0$ = 10 μM, and $[PMSO]_0$ = 50 μM; and for b, $[ABTS]_0$ = 200 μM and $[ferrate(VI)]_0$ = 10 μM. Error bars represent standard deviation between parallel experiments.

confirmed that the reaction of PAA (100 μM) and HSO_3^- (20 μM) was negligible in the first 5 s at pH 9.0 (data not shown). Therefore, HSO_3^-, PAA, and the target compound were mixed first, then ferrate(VI) was quickly added, and finally, the removal of the target compound was measured at 10 s. Note that HSO_3^- reacts very rapidly with ferrate(VI) through a single-electron transfer reaction[48] and thus leaves the activation of ferrate(VI) by H_2O_2 in PAA or PAA itself, if any, negligible. In this system, PAA still significantly promoted the removal of CBZ and PMSO by activated ferrate(VI) in 10 s. In sharp contrast, adding H_2O_2 (equivalent to the background H_2O_2 concentration in PAA solution) provided very limited acceleration for the degradation of CBZ and PMSO by ferrate(VI)−HSO_3^- (Figure 4a). These results provided unequivocal evidence that PAA enhanced ferrate(VI)

https://doi.org/10.1021/acs.est.2c02381
Environ. Sci. Technol. 2022, 56, 11683−11693

oxidation processes without being an activator because adding a weak activator (e.g., H_2O_2) could hardly affect contaminant removal by ferrate(VI)−HSO_3^- in such a short reaction time (10 s). Furthermore, when ferrate(VI) and HSO_3^- were added at a 5:1 molar ratio as in the experiments, intermediate high-valent iron was the main reactive species in the ferrate(VI)−HSO_3^- system as indicated by the literature.[48] Moreover, a 100% conversion yield of PMSO to $PMSO_2$ was also observed in the ferrate(VI)−HSO_3^--PAA system, suggesting that PAA did not change the main reactive species [i.e., Fe(IV)/Fe(V)] in ferrate(VI)−HSO_3^-. Thus, the enhancing effects of PAA on CBZ and PMSO removal by ferrate(VI)−HSO_3^- could only be attributed to its ability in strengthening Fe(IV)/Fe(V).

As a second approach, PAA was added into a ferrate(VI)-ABTS system (Figure 4b). It is well-documented that ferrate(VI) reacts with ABTS instantaneously through single-electron transfer and generates Fe(III) as the final product (eqs 5−7).[28,52] When ABTS is in excess, the fate of ferrate(VI) is dominated by oxidation of ABTS, while ferrate(VI) self-decay is negligible. If all the generated Fe(IV)/Fe(V) is also used for ABTS oxidation, rather than self-decay, each ferrate(VI) will oxidize three ABTS molecules. Nonetheless, Fe(IV)/Fe(V) self-decay always outcompetes their oxidation reaction, especially in phosphate buffer, resulting in a waste (or decrease in oxidation capacity) of the oxidant.[52,53] As a result, the stoichiometry between consumed ferrate(VI) and produced $ABTS^{\bullet+}$ is always a value between 1−3, depending on the buffer, molar ratio of ferrate(VI) and ABTS, and pH. Thus, the utilization percentage of Fe(IV)/Fe(V) in a ferrate(VI)-ABTS system can be calculated as eq 8.

$$\mathrm{Fe(VI)} + \mathrm{ABTS} \rightarrow \mathrm{Fe(V)} + \mathrm{ABTS}^{\bullet+} \quad (5)$$

$$\mathrm{Fe(V)} + \mathrm{ABTS} \rightarrow \mathrm{Fe(IV)} + \mathrm{ABTS}^{\bullet+} \quad (6)$$

$$\mathrm{Fe(IV)} + \mathrm{ABTS} \rightarrow \mathrm{Fe(III)} + \mathrm{ABTS}^{\bullet+} \quad (7)$$

$$\text{Fe(IV)/Fe(V) utilization efficiency} = \frac{[\mathrm{ABTS}^{\bullet+}]/\Delta[\text{ferrate (VI)}] - 1}{3 - 1} \quad (8)$$

Therefore, we spiked ferrate(VI) into test vails containing both PAA and ABTS and measured $ABTS^{\bullet+}$ formation. Consistent with the previous literature, in pH 7.0 phosphate buffer, the self-decay of Fe(V) totally dominated the fate of Fe(V), where the utilization efficiency of Fe(V)/Fe(IV) was near 0 (Figure S1). Under this condition, PAA did not cause any change (Figure S1), which is reasonable because we found that protonated PAA could not contribute to ferrate(VI) oxidation systems (Figure 1b−d). On the contrary, in pH 9.0 borate buffer, the $[ABTS^{\bullet+}]/\Delta[\text{ferrate(VI)}]$ ratio increased from 1.52 to 1.77, 1.88, 2.28, and 2.56 when the PAA concentration was increased from 0 to 10, 20, 50, and 100 μM, respectively (Figure 4b). Oppositely, background H_2O_2 and acetate were influenced by decreasing this ratio to 1.20 (Figure S2). In other words, the electron transfer efficiency between Fe(IV)/Fe(V) and ABTS (without the presence of PAA) was only 26.0%, with 74.0% wasted by rapid self-decay at pH 9.0. However, with addition of 100 μM PAA, 77.8% of Fe(IV)/Fe(V) oxidized ABTS, with only 22.2% loss to self-decay, suggesting that the oxidation outcompeted self-decay. This is another strong evidence that PAA strengthened Fe(IV)/Fe(V), rather than activating ferrate(VI), because activators like H_2O_2 will only compete with ABTS for high-valent iron instead of promoting the electron transfer between high-valent iron and ABTS.

Currently, there exists a knowledge gap on the possible interactions of PAA with Fe(IV)/Fe(V) species. Serrano-Plana et al. reported that PAA oxidized a mononuclear iron complex $[Fe^{II}(CF_3SO_3)_2(PyNMe_3)]$ to a high-valent iron-PAA complex {i.e., $[Fe^{v}(O)(OAc)(PyNMe_3)]^{2+}$}, which is 4 orders of magnitude more reactive than the Fe(V)-TAML complex, in terms of C−H bond cleavage of cyclohexane.[60] Although the lack of suitable instrumental techniques hindered the identification of the Fe(IV)/Fe(V)-PAA complexes in a ferrate(VI)-PAA system, thus far, based on the results presented above, we propose that some kinds of iron-PAA complexes were formed. These Fe(IV)/Fe(V)-PAA complexes should be more unstable and much more oxidative than the common hydroxide complexes of Fe(IV)/Fe(V). In addition, as the enhancing effect was only obvious at pH higher than the pK_a of PAA, we suspect that only deprotonated PAA could strongly complex with high-valent iron species.

PAA Loss in the Ferrate(VI)-PAA System. To monitor the fate of PAA in the ferrate(VI)-PAA system, here, we proposed a novel ABTS−DPD−KI method (in pH 7.0 phosphate buffer) for simultaneous quantification of ferrate(VI) and PAA (Figure 5). Briefly, excess ABTS selectively quenches the ferrate(VI) in

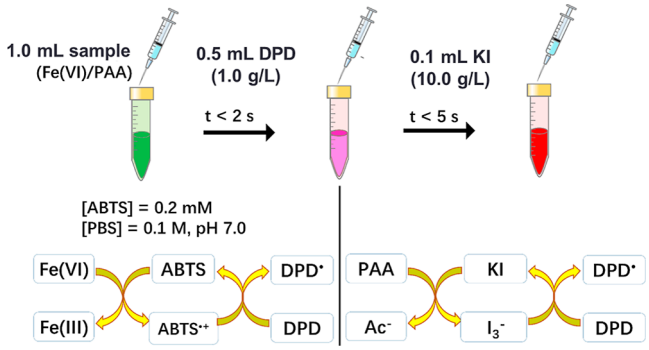

Figure 5. Illustration of the ABTS−KI−DPD method. PBS: phosphate buffer solution and Ac^-: acetate.

the sample and leaves PAA alone (the negligible reaction of ABTS or $ABTS^{\bullet+}$ with PAA at t < 60 s was confirmed by control experiments, Figure S3). The amount of $ABTS^{\bullet+}$ formed corresponds to the ferrate(VI) concentration.[52] The ferrate(VI) is reduced to Fe(III), which reacts extremely slowly with PAA at pH 7.0.[33] Then, DPD was added to convert green $ABTS^{\bullet+}$ to pink $DPD^{\bullet}$ immediately and to enable the KI−DPD method for PAA quantification upon addition of KI. Finally, the difference of absorbance at 515 nm ($DPD^{\bullet}$) before and after KI addition was used to calculate the PAA concentration. Control experiments confirmed that ABTS and H_2O_2 could not affect the KI−DPD method (Figure S4), and this novel method yielded the same standard calibration curve as that of the KI−DPD method for PAA alone (Figure S5).

By using the new ABTS−DPD−KI method, it was found that PAA loss, although less than ferrate(VI) loss, was actually not negligible in the ferrate(VI)-PAA system (Figure 3b). However, we did not perform further kinetic modeling on the PAA loss profile due to difficulties in estimating the rate constants for R12 and R13 (Table 1). As discussed above, (1)

https://doi.org/10.1021/acs.est.2c02381
Environ. Sci. Technol. 2022, 56, 11683−11693

PAA could change the reactivity and self-decay of Fe(IV)/Fe(V), (2) the possible formation of iron-PAA complexes could make the kinetic model more complicated, and (3) it is unclear currently whether PAA interacts with both or one of Fe(IV)/Fe(V). Furthermore, we also tried to measure Fe(II) by ferrozin for evaluating R12; however, no Fe(II) was detectable, probably due to the oxidation by ferrate(VI) (R7). Therefore, the kinetic model thus far is suitable for predicting ferrate(VI) decay in the presence of H_2O_2 or PAA/H_2O_2 and for use as an illustrative tool to understand the ferrate(VI)-PAA system.

Oxidation Product Comparison. The oxidation products (OPs) of CBZ by ferrate(VI)-PAA and ferrate(VI)−H_2O_2 were compared to evaluate the influence of PAA on the oxidation pathways by Fe(IV)/Fe(V). However, we found no obvious differences in the oxidation pathways by these two processes. OP251, OP253, OP267, and OP272 were identified in LC-HRMS (Figure S6), while OP269 and OP 285 were proposed as transient intermediates that could not be detected, as demonstrated by Hu et al. As Hu et al. reported, ferrate(VI) oxidation of CBZ was initiated by addition to the olefinic double bond on the seven-membered ring in the middle of the CBZ molecule.[61] Two oxidation pathways were reported for this first-step reaction by Hu and co-workers: (1) cleavage of the double bond with formation of two aldehyde groups and (2) formation of one carbonyl group in place of the double bond without cleavage of the seven-membered ring. Nonetheless, only the former product was observed in this study (Figure 6). Then, dehydration between the amine group and aldehyde group happened, either before or after the further oxidation of one aldehyde group to a carboxylic group, forming a N-containing heterocycle.[61] Another pathway initiated by the epoxidation of the olefinic double bond was also observed.[62]

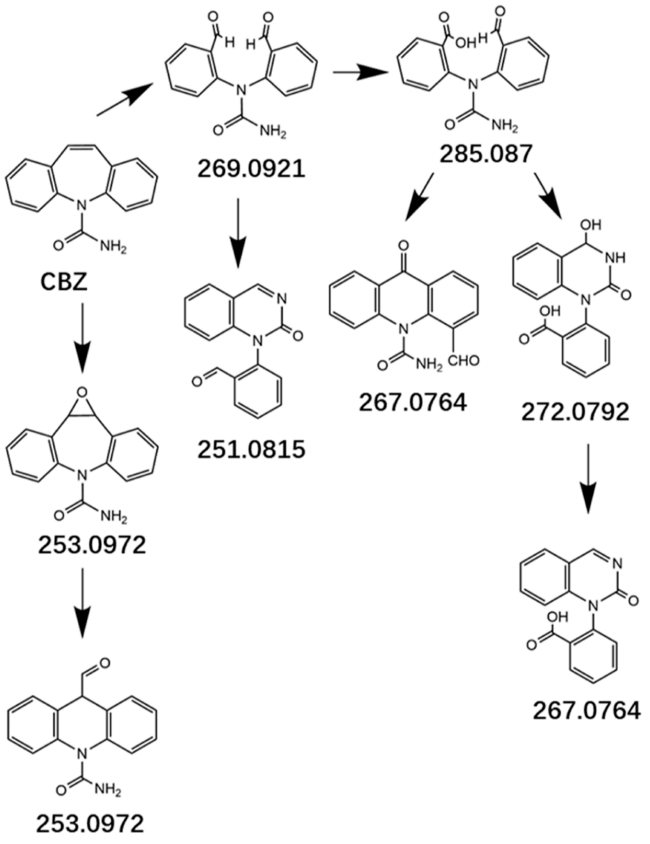

Figure 6. Oxidation products of CBZ by ferrate(VI)-PAA or ferrate(VI)−H_2O_2. *m/z* values [monoisotopic, protonated fragments in ESI(+)] for each compound are presented.

Effects of the Water Matrix on Ferrate(VI)-PAA and Ferrate(VI) Alone. The impacts of chloride (Cl^-), bicarbonate (HCO_3^-), phosphate ($HPO_4^{2-}/H_2PO_4^-$), and HA on the ferrate(VI)-PAA system were studied (Figures S7−S10). Chloride (1−20 mM) had a negligible impact on CBZ removal (Figure S7). This is consistent with the result of Luo et al., who showed that chloride could only affect the ferrate(VI) system when its concentration was high enough to change the ionic strength.[46] Phosphate (5−10 mM) inhibited CBZ removal by ferrate(VI)-PAA (Figure S8). Huang et al. also reported that phosphate weakened the oxidation capacity of ferrate(VI), probably through complexing with Fe(V).[53] HA (5−20 mg/L) did not affect CBZ removal by ferrate(VI)-PAA or ferrate(VI) alone (Figure S9). This conclusion is different from that of Feng et al., who found that HA (1−30 mg/L) had a negative impact on removal of fluoroquinolone antibiotics by ferrate(VI).[63] This discrepancy could be attributed to the different target compounds and buffers that affect the reactivity rates of Fe(V)/Fe(IV) species.

Bicarbonate slightly suppressed CBZ removal by both ferrate(VI)-PAA and ferrate(VI) alone in this study (Figure S10a). For ferrate(VI)-only systems, Feng et al. found that 5 mM bicarbonate had a slight enhancing effect on the removal of fluoroquinolone antibiotics by ferrate(VI).[63] Luo et al. demonstrated that bicarbonate (0.25 M) enhanced sulfamethoxazole removal by ferrate(VI), while it did not affect the removal of CBZ and naproxen.[46] It is noteworthy that these two studies used phosphate buffer as a control for the comparison with the bicarbonate system, while phosphate itself could act as a major inhibitor. Consequently, we systematically compared CBZ oxidation by ferrate(VI) alone in borate, phosphate, bicarbonate buffers, and their combinations (Figure S10b). The order for CBZ removal is borate > bicarbonate (with or without borate) > phosphate (with or without bicarbonate). Therefore, bicarbonate and phosphate are both inhibitors for ferrate(VI) oxidation, though phosphate is a stronger one.

Environmental Significance and Implications. Ferrate(VI) and PAA are two green oxidants that have recently garnered extensive research interests owing to their low tendency to form harmful DBPs. This study confirms that the combination of PAA and ferrate(VI) leads to more rapid micropollutant abatement performance. The activation of ferrate(VI) by PAA is very limited. Rather, for the first time, the potential of PAA in interacting with Fe(IV)/Fe(V) is proposed. The electron transfer efficiency between ferrate(VI) and micropollutants is limited by the rapid decay of Fe(IV)/Fe(V). The simultaneous combination of PAA with ferrate(VI) can greatly strengthen Fe(IV)/Fe(V) and let their oxidation outperform the self-decay. We used CBZ as a target compound and showed that its 2 min removal was enhanced by more than 60% by the combination of ferrate(VI) and PAA at pH 9.0. Although BA was still resistant to ferrate oxidation in the presence of PAA, most PPCPs have complicated structures with reactive sites for high-valent iron.[14] Thus, an enhancement of PPCP removal by ferrate(VI)-PAA is expected, especially for alkaline wastewater treatment (e.g., decentralized urine treatment, industrial wastewater treatment).

https://doi.org/10.1021/acs.est.2c02381
Environ. Sci. Technol. 2022, 56, 11683−11693

Results of this study also open the possibility to apply PAA to other ferrate(VI)-related AOPs and possibly to biomimetic synthesis of high-valent iron complexes. Additionally, this study shows that advanced oxidation can be achieved through electron transfer promotion, even when the direct activation is limited, which has implications for understanding other metal-based AOPs. For example, the synergistic oxidation mechanisms of several metal-peroxide AOPs are under debate, including the ferrate(VI)-peroxymonosulfate (PMS),[64] Co(II)-PMS,[65] and Co(II)-PAA systems.[35] Recently, the activation reaction mechanism has been challenged by the complexation-enhanced electron transfer mechanism.[35,65] To elucidate the roles of the two mechanisms, the experimental design employed in this study (e.g., validation of probe compounds and comparison of oxidant decay in the presence and absence of potential activators) could be exploited. Overall, the novel mechanism and methodology in this study should provide valuable insights for future research on metal-peroxide types of AOPs.

■ ASSOCIATED CONTENT

Supporting Information

The Supporting Information is available free of charge at https://pubs.acs.org/doi/10.1021/acs.est.2c02381.

Analytical methods, kinetic modeling, quenching of H_2O_2 in PAA solution, validation of the ABTS−DPD−KI method, ABTS oxidation by ferrate(VI) and ferrate(VI)/PAA at pH 7.0, oxidation products of CBZ, and water matrix effects (PDF)

■ AUTHOR INFORMATION

Corresponding Authors

Virender K. Sharma − *Department of Environment and Occupational Health, School of Public Health, Texas A&M University, College Station, Texas 77843, United States;* orcid.org/0000-0002-5980-8675; Email: vsharma@tamu.edu

Ching-Hua Huang − *School of Civil and Environmental Engineering, Georgia Institute of Technology, Atlanta, Georgia 30332, United States;* orcid.org/0000-0002-3786-094X; Email: ching-hua.huang@ce.gatech.edu

Authors

Junyue Wang − *School of Civil and Environmental Engineering, Georgia Institute of Technology, Atlanta, Georgia 30332, United States;* orcid.org/0000-0002-3752-1358

Juhee Kim − *School of Civil and Environmental Engineering, Georgia Institute of Technology, Atlanta, Georgia 30332, United States*

Daniel C. Ashley − *Department of Chemistry and Biochemistry, Spelman College, Atlanta, Georgia 30314, United States;* orcid.org/0000-0002-8838-4269

Complete contact information is available at: https://pubs.acs.org/10.1021/acs.est.2c02381

Notes

The authors declare no competing financial interest.

■ ACKNOWLEDGMENTS

This work was supported by the National Science Foundation Grants CHE-2108701 and CHE-2107967. Any opinions, findings, and conclusions or recommendations expressed in this material are those of the authors and do not necessarily reflect the views of the National Science Foundation. The authors are grateful for the facility assistance from Dr. Chaoyang Huang and valuable suggestions from Dr. Cong Luo, Yanghua Duan, Qi Shi, Allen Mao, and Song Su.

■ REFERENCES

(1) von Gunten, U. Oxidation processes in water treatment: Are we on track? *Environ. Sci. Technol.* **2018**, *52*, 5062−5075.

(2) Deborde, M.; von Gunten, U. Reactions of chlorine with inorganic and organic compounds during water treatment-Kinetics and mechanisms: a critical review. *Water Res.* **2008**, *42*, 13−51.

(3) Mangalgiri, K. P.; Patton, S.; Wu, L.; Xu, S.; Ishida, K. P.; Liu, H. Optimizing potable water reuse systems: Chloramines or hydrogen peroxide for UV-based advanced oxidation process? *Environ. Sci. Technol.* **2019**, *53*, 13323−13331.

(4) von Gunten, U. Ozonation of drinking water: Part I. Oxidation kinetics and product formation. *Water Res.* **2003**, *37*, 1443−1467.

(5) Rougé, V.; Allard, S.; Croué, J. P.; von Gunten, U. In situ formation of free chlorine during ClO2 treatment: Implications on the formation of disinfection byproducts. *Environ. Sci. Technol.* **2018**, *52*, 13421−13429.

(6) Ike, I. A.; Karanfil, T.; Cho, J.; Hur, J. Oxidation byproducts from the degradation of dissolved organic matter by advanced oxidation processes - A critical review. *Water Res.* **2019**, *164*, 114929.

(7) Bond, T.; Huang, J.; Templeton, M. R.; Graham, N. Occurrence and control of nitrogenous disinfection by-products in drinking water–A review. *Water Res.* **2011**, *45*, 4341−4354.

(8) Chuang, Y. H.; McCurry, D. L.; Tung, H. H.; Mitch, W. A. Formation pathways and trade-offs between haloacetamides and haloacetaldehydes during combined chlorination and chloramination of lignin phenols and natural waters. *Environ. Sci. Technol.* **2015**, *49*, 14432−14440.

(9) Huang, H.; Wu, Q. Y.; Hu, H. Y.; Mitch, W. A. Dichloroacetonitrile and dichloroacetamide can form independently during chlorination and chloramination of drinking waters, model organic matters, and wastewater effluents. *Environ. Sci. Technol.* **2012**, *46*, 10624−10631.

(10) Krasner, S. W.; Mitch, W. A.; McCurry, D. L.; Hanigan, D.; Westerhoff, P. Formation, precursors, control, and occurrence of nitrosamines in drinking water: a review. *Water Res.* **2013**, *47*, 4433−4450.

(11) Park, S.-H.; Wei, S.; Mizaikoff, B.; Taylor, A. E.; Favero, C.; Huang, C.-H. Degradation of amine-based water treatment polymers during chloramination as N-Nitrosodimethylamine (NDMA) precursors. *Environ. Sci. Technol.* **2009**, *43*, 1360−1366.

(12) Yang, J.; Dong, Z.; Jiang, C.; Wang, C.; Liu, H. An overview of bromate formation in chemical oxidation processes: Occurrence, mechanism, influencing factors, risk assessment, and control strategies. *Chemosphere* **2019**, *237*, 124521.

(13) McCurry, D. L.; Quay, A. N.; Mitch, W. A. Ozone promotes chloropicrin formation by oxidizing amines to nitro compounds. *Environ. Sci. Technol.* **2016**, *50*, 1209−1217.

(14) Sharma, V. K.; Chen, L.; Zboril, R. Review on high valent FeVI (Ferrate): A sustainable green oxidant in organic chemistry and transformation of pharmaceuticals. *ACS Sustainable Chem. Eng.* **2015**, *4*, 18−34.

(15) Sharma, V. K.; Zboril, R.; Varma, R. S. Ferrates: Greener oxidants with multimodal action in water treatment technologies. *Acc. Chem. Res.* **2015**, *48*, 182−191.

(16) Sharma, V. K.; Feng, M.; Dionysiou, D. D.; Zhou, H.-C.; Jinadatha, C.; Manoli, K.; Smith, M. F.; Luque, R.; Ma, X.; Huang, C.-H. Reactive high-valent iron intermediates in enhancing treatment of water by ferrate. *Environ. Sci. Technol.* **2022**, *56*, 30−47.

(17) Ao, X. W.; Eloranta, J.; Huang, C. H.; Santoro, D.; Sun, W. J.; Lu, Z. D.; Li, C. Peracetic acid-based advanced oxidation processes for

decontamination and disinfection of water: A review. *Water Res.* **2021**, *188*, 116479.
(18) Kim, J.; Huang, C.-H. Reactivity of peracetic acid with organic compounds: A critical review. *ACS ES&T Water* **2020**, *1*, 15−33.
(19) Sun, P.; Zhang, T.; Mejia-Tickner, B.; Zhang, R.; Cai, M.; Huang, C. H. Rapid disinfection by peracetic acid combined with UV irradiation. *Environmental Science & Technology Letters* **2018**, *5*, 400−404.
(20) Zhang, T.; Wang, T.; Mejia-Tickner, B.; Kissel, J.; Xie, X.; Huang, C. H. Inactivation of bacteria by peracetic acid combined with ultraviolet irradiation: Mechanism and optimization. *Environ. Sci. Technol.* **2020**, *54*, 9652−9661.
(21) Hu, L.; Page, M. A.; Sigstam, T.; Kohn, T.; Mariñas, B. J.; Strathmann, T. J. Inactivation of bacteriophage MS2 with potassium ferrate(VI). *Environ. Sci. Technol.* **2012**, *46*, 12079−12087.
(22) Sharma, V. K. Disinfection performance of Fe(VI) in water and wastewater: a review. *Water Sci. Technol.* **2007**, *55*, 225−232.
(23) Dunkin, N.; Weng, S.; Schwab, K. J.; McQuarrie, J.; Bell, K.; Jacangelo, J. G. Comparative inactivation of murine norovirus and MS2 bacteriophage by peracetic acid and monochloramine in municipal secondary wastewater fffluent. *Environ. Sci. Technol.* **2017**, *51*, 2972−2981.
(24) Baum, J. C.; Feng, M.; Guo, B.; Huang, C.-H.; Sharma, V. K. Generation of Iron(IV) in the oxidation of amines by ferrate(VI): Theoretical insight and implications in oxidizing pharmaceuticals. *ACS ES&T Water* **2021**, *1*, 1932−1940.
(25) Feng, M.; Baum, J. C.; Nesnas, N.; Lee, Y.; Huang, C. H.; Sharma, V. K. Oxidation of sulfonamide antibiotics of six-membered heterocyclic moiety by ferrate(VI): Kinetics and mechanistic insight into SO2 extrusion. *Environ. Sci. Technol.* **2019**, *53*, 2695−2704.
(26) Du, P.; Liu, W.; Cao, H.; Zhao, H.; Huang, C. H. Oxidation of amino acids by peracetic acid: Reaction kinetics, pathways and theoretical calculations. *Water Res.: X* **2018**, *1*, 100002.
(27) Zhang, K.; Zhou, X.; Du, P.; Zhang, T.; Cai, M.; Sun, P.; Huang, C. H. Oxidation of beta-lactam antibiotics by peracetic acid: Reaction kinetics, product and pathway evaluation. *Water Res.* **2017**, *123*, 153−161.
(28) Lee, Y.; Kissner, R.; von Gunten, U. Reaction of ferrate(VI) with ABTS and self-decay of ferrate(VI): kinetics and mechanisms. *Environ. Sci. Technol.* **2014**, *48*, 5154−5162.
(29) Wang, S.; Shao, B.; Qiao, J.; Guan, X. Application of Fe(VI) in abating contaminants in water: State of art and knowledge gaps. *Front. Environ. Sci. Eng.* **2020**, *15*, 80.
(30) Zhu, J.; Yu, F.; Meng, J.; Shao, B.; Dong, H.; Chu, W.; Cao, T.; Wei, G.; Wang, H.; Guan, X. Overlooked role of Fe(IV) and Fe(V) in organic contaminant oxidation by Fe(VI). *Environ. Sci. Technol.* **2020**, *54*, 9702−9710.
(31) Cai, M.; Sun, P.; Zhang, L.; Huang, C. H. UV/Peracetic acid for degradation of pharmaceuticals and reactive species evaluation. *Environ. Sci. Technol.* **2017**, *51*, 14217−14224.
(32) Zhang, T.; Huang, C. H. Modeling the kinetics of UV/peracetic acid advanced oxidation process. *Environ. Sci. Technol.* **2020**, *54*, 7579−7590.
(33) Kim, J.; Zhang, T.; Liu, W.; Du, P.; Dobson, J. T.; Huang, C. H. Advanced oxidation process with peracetic acid and Fe(II) for contaminant degradation. *Environ. Sci. Technol.* **2019**, *53*, 13312−13322.
(34) Kim, J.; Wang, J.; Ashley, D. C.; Sharma, V. K.; Huang, C. H. Enhanced degradation of micropollutants in a peracetic Acid-Fe(III) system with picolinic acid. *Environ. Sci. Technol.* **2022**, *56*, 4437−4446.
(35) Zhao, Z.; Li, X.; Li, H.; Qian, J.; Pan, B. New insights into the activation of peracetic acid by Co(II): Role of Co(II)-peracetic acid complex as the dominant intermediate oxidant. *ACS ES&T Engg* **2021**, *1*, 1432−1440.
(36) Kim, J.; Du, P.; Liu, W.; Luo, C.; Zhao, H.; Huang, C. H. Cobalt/peracetic acid: advanced oxidation of aromatic organic compounds by acetylperoxyl radicals. *Environ. Sci. Technol.* **2020**, *54*, 5268−5278.
(37) Liu, B.; Guo, W.; Jia, W.; Wang, H.; Zheng, S.; Si, Q.; Zhao, Q.; Luo, H.; Jiang, J.; Ren, N. Insights into the oxidation of organic contaminants by Co(II) activated peracetic acid: The overlooked role of high-valent cobalt-oxo species. *Water Res.* **2021**, *201*, 117313.
(38) Li, R.; Manoli, K.; Kim, J.; Feng, M.; Huang, C. H.; Sharma, V. K. Peracetic acid-Ruthenium(III) oxidation process for the degradation of micropollutants in water. *Environ. Sci. Technol.* **2021**, *55*, 9150−9160.
(39) Wang, J.; Wang, Z.; Cheng, Y.; Cao, L.; Bai, F.; Yue, S.; Xie, P.; Ma, J. Molybdenum disulfide (MoS2): A novel activator of peracetic acid for the degradation of sulfonamide antibiotics. *Water Res.* **2021**, *201*, 117291.
(40) Zhang, L.; Chen, J.; Zhang, Y.; Yu, Z.; Ji, R.; Zhou, X. Activation of peracetic acid with cobalt anchored on 2D sandwich-like MXenes (Co@MXenes) for organic contaminant degradation: High efficiency and contribution of acetylperoxyl radicals. *Appl. Catal., B* **2021**, *297*, 120475.
(41) Liu, B.; Guo, W.; Jia, W.; Wang, H.; Si, Q.; Zhao, Q.; Luo, H.; Jiang, J.; Ren, N. Novel nonradical oxidation of sulfonamide antibiotics with Co(II)-Doped g-C3N4-activated peracetic acid: role of high-valent cobalt-oxo species. *Environ. Sci. Technol.* **2021**, *55*, 12640−12651.
(42) Wang, J.; Xiong, B.; Miao, L.; Wang, S.; Xie, P.; Wang, Z.; Ma, J. Applying a novel advanced oxidation process of activated peracetic acid by CoFe2O4 to efficiently degrade sulfamethoxazole. *Appl. Catal., B* **2021**, *280*, 119422.
(43) Zhang, X.; Feng, M.; Luo, C.; Nesnas, N.; Huang, C. H.; Sharma, V. K. Effect of metal ions on oxidation of micropollutants by ferrate(VI): enhancing role of Fe(IV) species. *Environ. Sci. Technol.* **2021**, *55*, 623−633.
(44) Manoli, K.; Nakhla, G.; Feng, M.; Sharma, V. K.; Ray, A. K. Silica gel-enhanced oxidation of caffeine by ferrate(VI). *Chem. Eng. J.* **2017**, *330*, 987−994.
(45) Feng, M.; Cizmas, L.; Wang, Z.; Sharma, V. K. Activation of ferrate(VI) by ammonia in oxidation of flumequine: Kinetics, transformation products, and antibacterial activity assessment. *Chem. Eng. J.* **2017**, *323*, 584−591.
(46) Luo, C.; Feng, M.; Sharma, V. K.; Huang, C. H. Oxidation of pharmaceuticals by ferrate(VI) in hydrolyzed urine: effects of major inorganic constituents. *Environ. Sci. Technol.* **2019**, *53*, 5272−5281.
(47) Shao, B.; Dong, H.; Sun, B.; Guan, X. Role of ferrate(IV) and ferrate(V) in activating ferrate(VI) by calcium sulfite for enhanced oxidation of organic contaminants. *Environ. Sci. Technol.* **2019**, *53*, 894−902.
(48) Shao, B.; Dong, H.; Feng, L.; Qiao, J.; Guan, X. Influence of [sulfite]/[Fe(VI)] molar ratio on the active oxidants generation in Fe(VI)/sulfite process. *J. Hazard. Mater.* **2020**, *384*, 121303.
(49) Manoli, K.; Li, R.; Kim, J.; Feng, M.; Huang, C.-H.; Sharma, V. K. Ferrate(VI)-peracetic acid oxidation process: Rapid degradation of pharmaceuticals in water. *Chem. Eng. J.* **2022**, *429*, 132384.
(50) Luo, C.; Feng, M.; Sharma, V. K.; Huang, C.-H. Revelation of ferrate(VI) unimolecular decay under alkaline conditions: Investigation of involvement of Fe(IV) and Fe(V) species. *Chem. Eng. J.* **2020**, *388*, 124134.
(51) Feng, M.; Jinadatha, C.; McDonald, T. J.; Sharma, V. K. Accelerated oxidation of organic contaminants by ferrate(VI): The overlooked role of reducing additives. *Environ. Sci. Technol.* **2018**, *52*, 11319−11327.
(52) Luo, C.; Sadhasivan, M.; Kim, J.; Sharma, V. K.; Huang, C. H. Revelation of Fe(V)/Fe(IV) Involvement in the Fe(VI)-ABTS System: Kinetic Modeling and Product Analysis. *Environ. Sci. Technol.* **2021**, *55*, 3976−3987.
(53) Huang, Z. S.; Wang, L.; Liu, Y. L.; Jiang, J.; Xue, M.; Xu, C. B.; Zhen, Y. F.; Wang, Y. C.; Ma, J. Impact of phosphate on ferrate oxidation of organic compounds: An underestimated oxidant. *Environ. Sci. Technol.* **2018**, *52*, 13897−13907.
(54) Chuang, Y. H.; Chen, S.; Chinn, C. J.; Mitch, W. A. Comparing the UV/monochloramine and UV/free chlorine advanced oxidation orocesses (AOPs) to the UV/Hydrogen peroxide AOP under

scenarios relevant to potable reuse. *Environ. Sci. Technol.* **2017**, *51*, 13859−13868.
(55) Zhang, T.; Huang, C. H. Simultaneous quantification of peracetic acid and hydrogen peroxide in different water matrices using HPLC-UV. *Chemosphere* **2020**, *257*, 127229.
(56) Sharma, V. K. Oxidation of inorganic contaminants by ferrates (VI, V, and IV)–kinetics and mechanisms: a review. *J. Environ. Manage.* **2011**, *92*, 1051−1073.
(57) Bielski, B. H. J.; Sharma, V. K.; Czapski, G. Reactivity of ferrate(V) with carboxylic acids: A pre-mix pulse radiolysis study. *Radiat. Phys. Chem.* **1994**, *44*, 479−484.
(58) Zhang, R.; Sun, P.; Boyer, T. H.; Zhao, L.; Huang, C. H. Degradation of pharmaceuticals and metabolite in synthetic human urine by UV, UV/H2O2, and UV/PDS. *Environ. Sci. Technol.* **2015**, *49*, 3056−3066.
(59) Wang, J.; Wan, Y.; Ding, J.; Wang, Z.; Ma, J.; Xie, P.; Wiesner, M. R. Thermal activation of peracetic acid in aquatic solution: The mechanism and application to degrade sulfamethoxazole. *Environ. Sci. Technol.* **2020**, *54*, 14635−14645.
(60) Serrano-Plana, J.; Oloo, W. N.; Acosta-Rueda, L.; Meier, K. K.; Verdejo, B.; García-España, E.; Basallote, M. G.; Münck, E.; Que, L., Jr.; Company, A.; Costas, M. Trapping a highly reactive nonheme iron intermediate that oxygenates strong C-H bonds with stereoretention. *J. Am. Chem. Soc.* **2015**, *137*, 15833−15842.
(61) Hu, L.; Martin, H. M.; Arce-Bulted, O.; Sugihara, M. N.; Keating, K.; Strathmann, T. J. Oxidation of carbamazepine by Mn(VII) and Fe(VI): Reaction kinetics and mechanism. *Environ. Sci. Technol.* **2009**, *43*, 509−515.
(62) Li, Y.; Yang, Y.; Lei, J.; Liu, W.; Tong, M.; Liang, J. The degradation pathways of carbamazepine in advanced oxidation process: A mini review coupled with DFT calculation. *Sci. Total Environ.* **2021**, *779*, 146498.
(63) Feng, M.; Wang, X.; Chen, J.; Qu, R.; Sui, Y.; Cizmas, L.; Wang, Z.; Sharma, V. K. Degradation of fluoroquinolone antibiotics by ferrate(VI): Effects of water constituents and oxidized products. *Water Res.* **2016**, *103*, 48−57.
(64) Feng, M.; Cizmas, L.; Wang, Z.; Sharma, V. K. Synergistic effect of aqueous removal of fluoroquinolones by a combined use of peroxymonosulfate and ferrate(VI). *Chemosphere* **2017**, *177*, 144−148.
(65) Li, H.; Zhao, Z.; Qian, J.; Pan, B. Are Free Radicals the Primary Reactive Species in Co(II)-Mediated Activation of Peroxymonosulfate? New Evidence for the Role of the Co(II)-Peroxymonosulfate Complex. *Environ. Sci. Technol.* **2021**, *55*, 6397−6406.

https://doi.org/10.1021/acs.est.2c02381
Environ. Sci. Technol. 2022, 56, 11683−11693